Investigation of Band Structure in Strained Single Crystalline $Si_{1-X}Sn_X$

ECS Transactions, 109 (4) 359-366 (2022)
10.1149/10904.0359ecst ©The Electrochemical Society

Investigation of Band Structure in Strained Single Crystalline $Si_{1-x}Sn_x$

K. Sahara[1], R. Yokogawa[1, 2], Y. Shibayama[1], Y. Hibino[2, 3],
M. Kurosawa[4], and A. Ogura[1, 2]

[1]School of Science and Technology, Meiji University, 1-1-1 Higashimita, Tama-ku, Kawasaki, Kanagawa 214-8571, Japan
[2]Meiji Renewable Energy Laboratory, Meiji University, 1-1-1 Higashimita, Tama-ku, Kawasaki, Kanagawa 214-8571, Japan
[3]National Institute of Technology, Sasebo College, Okisin-machi, Sasebo, Nagasaki 857-1171, Japan
[4]Graduate School of Engineering, Nagoya University, Furo-cho, Chikusa-ku, Nagoya, 464-8603, Japan
Corresponding author: ce211027@meiji.ac.jp

We evaluated the optical properties and the band structure of strained single crystalline $Si_{1-x}Sn_x$ using spectroscopic ellipsometry. The results suggest a reduction of the band gap at the Γ point and the formation of an optical transition by Van-Hove singularity with higher Sn fraction. In addition, since the reduction of the band gap with increasing Sn fraction at the Γ point is larger than at other points, it is expected the indirect transition type $Si_{1-x}Sn_x$ used in this study may eventually change to the direct transition type. Although higher Sn fraction are required to achieve direct transition type $Si_{1-x}Sn_x$, the band structure of strained single crystal $Si_{1-x}Sn_x$ was experimentally clarified.

Introduction

Silicon tin (SiSn) alloys are attractive candidates for the next-generation group-IV semiconductors because of the high affinity with Si-based semiconductor devices and the ability to control their energy band gap by Sn fraction [1-5]. In addition, SiSn alloys are expected to be applied for the near-infrared optical devices since it is predicted to exhibit direct band-gap appropriate for the optical communication with sufficient Sn fraction [6-8]. Although the correlation between Sn fraction and the band-gap of SiSn alloys has been reported using several calculations, there are few reports of experimental results. In addition, polycrystalline or amorphous SiSn is used for most of

the optical evaluation [9-11] owing to the difficulty of crystal growth [12].

In this study, we evaluated the optical properties to investigate the band structure of strained single crystalline $Si_{1-x}Sn_x$ using spectroscopic ellipsometry.

Experimental method

Strained $Si_{1-x}Sn_x$ thin films (target thickness: 50 nm) were grown on Si substrate by molecular beam epitaxy (MBE), and the epitaxial films were confirmed by X-ray diffraction (XRD) two-dimensional reciprocal space mapping (2DRSM) [13]. The Sn fraction and strain were determined by 2DRSM. The Sn fraction x of $Si_{1-x}Sn_x$ thin film samples used in this study were determined as 0.005, 0.009, 0.018, 0.022, and 0.06. Table 1 summarizes the structural parameters of $Si_{1-x}Sn_x$ thin film samples. The spectroscopic ellipsometry measurements were performed, because it is powerful for evaluating the band structure of semiconductor materials since the complex dielectric functions of the semiconductor include much information about the electronic band structure [14, 15]. The measurement conditions were an incident angle of 70°, using a 70 W xenon lamp with a wavelength range of 200 to 1600 nm for the light source.

Table 1. Structural parameters of $Si_{1-x}Sn_x$ thin film samples.

Sn fraction (%)	Deposition Temperature (℃)	Sn precipitation
0.5	**300**	**Yes**
0.9	**280**	**Yes**
1.8	**260**	**No**
2.2	**260**	**Yes**
6.0	**220**	**Yes**

Results and Discussion

Figure 1 shows the experimental Ψ and Δ data and the model fits for $Si_{1-x}Sn_x$ (x= 0.005 - 0.06). To evaluate the optical properties of the $Si_{1-x}Sn_x$ film layer, Ψ and Δ data were modeled using three layers structure, including the native oxide layer, the $Si_{1-x}Sn_x$ film layer, and the Si substrate. The $Si_{1-x}Sn_x$ layers are modeled using Tauc-Lorentz functions, which ensure Kramers-Kronig consistency between the real and imaginary

parts of the complex dielectric functions. From Fig. 1, the model fits are sufficiently consistent with the experimental Ψ and Δ data for all $Si_{1-x}Sn_x$ thin film samples, and the shape of Ψ and Δ data changes with increasing Sn fraction.

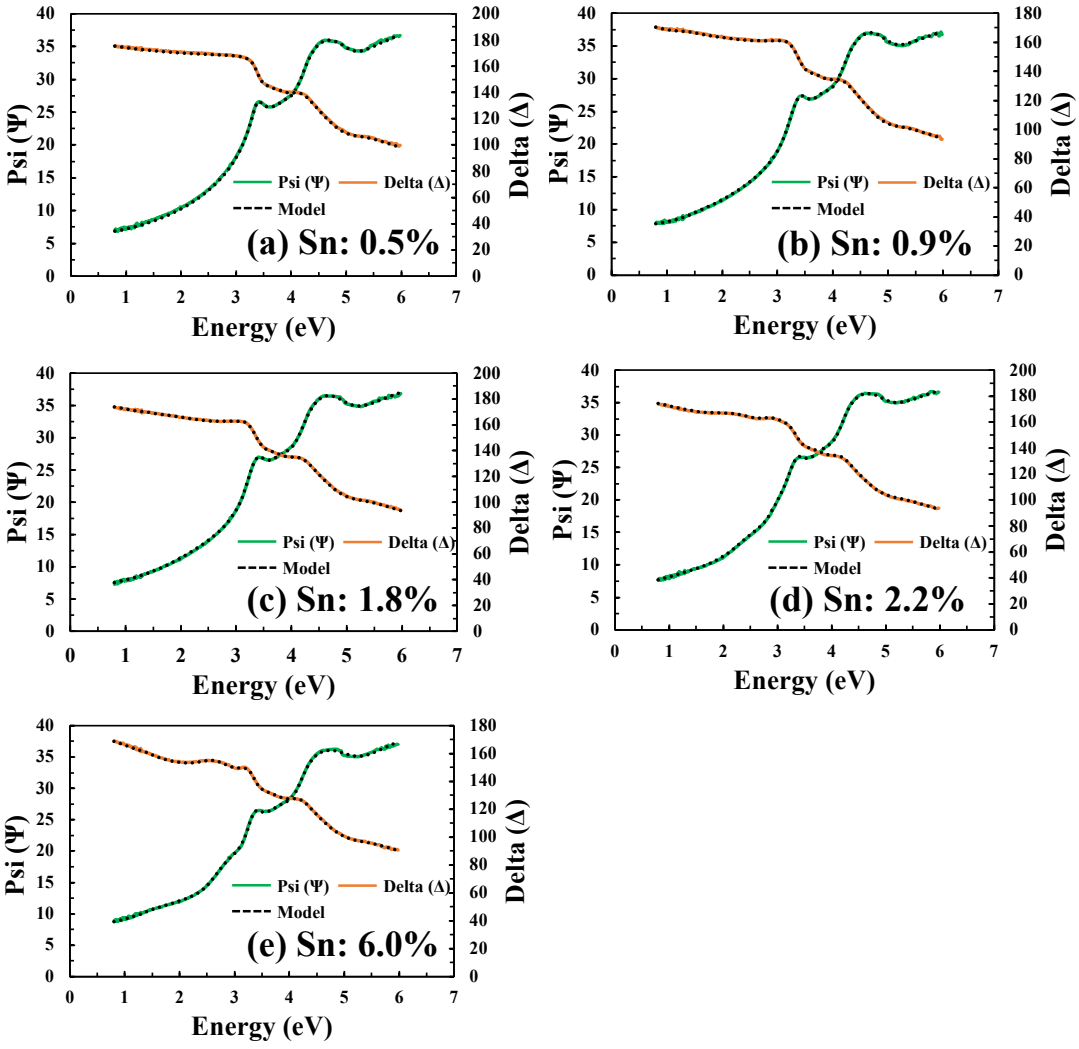

Figure 1. Experimental Ψ and Δ data and model fits of $Si_{1-x}Sn_x$ alloys for *x:* (a) 0.005, (b) 0.009, (c) 0.018, (d) 0.022 and (e) 0.06.

Figure 2 shows real part and imaginary part of the complex dielectric functions for $Si_{1-x}Sn_x$ (x= 0.005 - 0.06) and pure-Si, respectively. From Fig. 2, it can be confirmed that the spectral shift with increasing Sn fraction and the peaks appearance around 1.8 eV and 2.8 eV for the samples with high Sn fraction (x= 0.022 and 0.06). The peak shift with the addition of Sn is similar to the results for strained silicon germanium (SiGe) [16] and strained germanium tin (GeSn) [17], which are also alloy semiconductors.

In Fig. 2, the sharp peaks due to direct band transitions are known as critical points (CPs). In the case of Si, E'_0, optical transitions around Γ point, and E_1, optical

transitions around Λ point between Γ point and L point, respectively, both CP energies are around 3.4 eV [18]. In addition, it has been shown in theoretical predictions that the reduction of band gap at Γ point is more apparent than those at the L and X points with the addition of Sn [4, 5]. Therefore, it can be considered that the peak at 2.8 eV indicates the separation of the E'_0 and E_1 CP energies due to the change in the band gap at the Γ point with the addition of Sn. Taking into account the theoretical prediction of $Si_{1-x}Sn_x$ changes from indirect to direct transition types with the addition of Sn, this result is reasonable [1-5]. However, the peak appearance below 2.0 eV is unique optical transition to $Si_{1-x}Sn_x$, which is not found in Si.

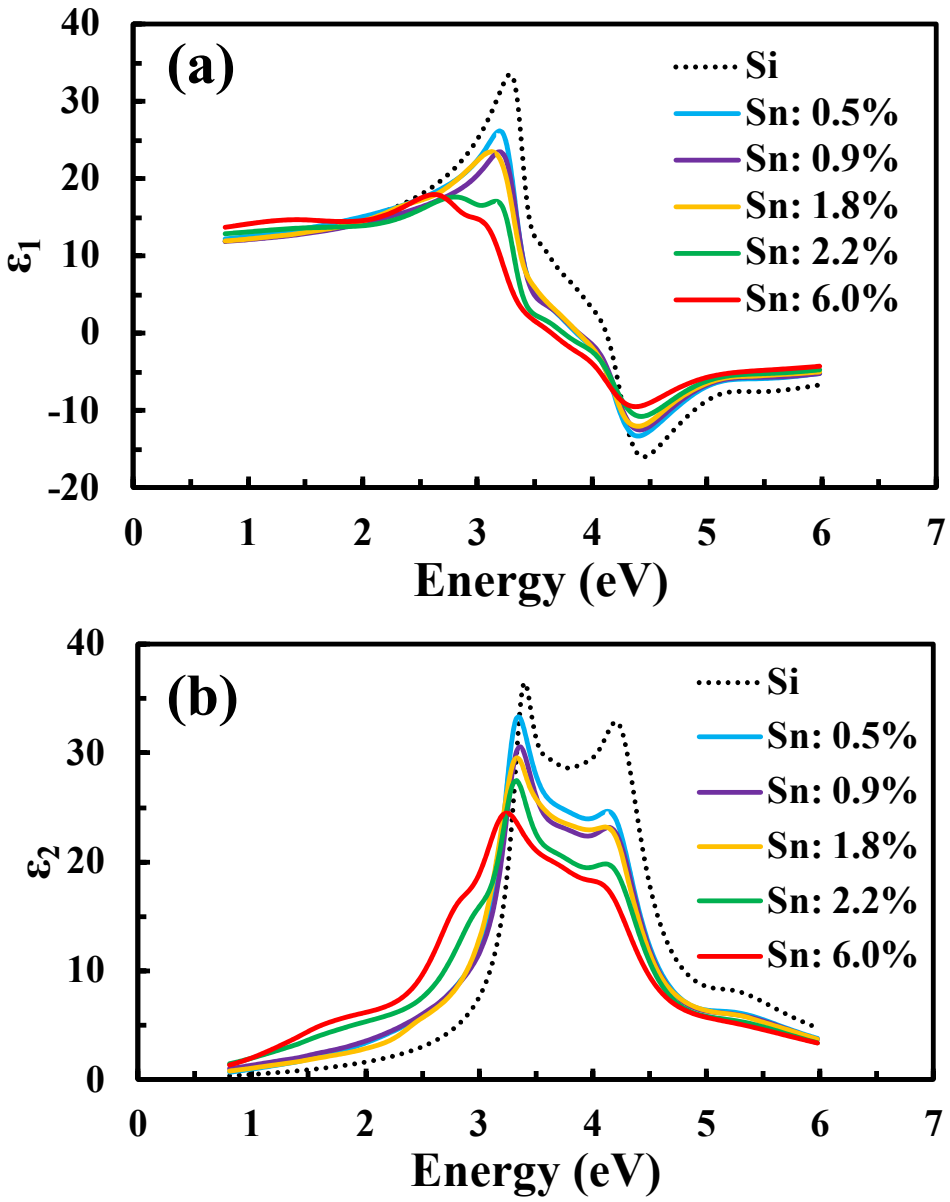

Figure 2. Complex dielectric function of pure Si and $Si_{1-x}Sn_x$ alloys for x= 0.005, 0.009, 0.018, 0.022 and 0.06. (a) Real part (ε_1) and (b) Imaginary part (ε_2).

Figure 3 shows the second derivatives of imaginary parts (ε_2) of the complex dielectric function for $Si_{1-x}Sn_x$ (x= 0.022 and 0.06) and pure Si with an energy of (a) 0.8 to 5.8 eV and (b) 0.8 to 2.8 eV. From Fig. 3(a), it can be confirmed that E'_0, E_1, and E_2 CPs are shifted with increasing Sn fraction, and each energy shift is different. In addition, we found the intensity of the peak appearing around 1.8 eV increases slightly and the peak shifts with increasing Sn fraction. These behaviors are similar to E'_0 CP. Therefore, the peaks appear around 1.8 eV suggest forming new optical transitions by Van-Hove singularity with increasing Sn composition [19].

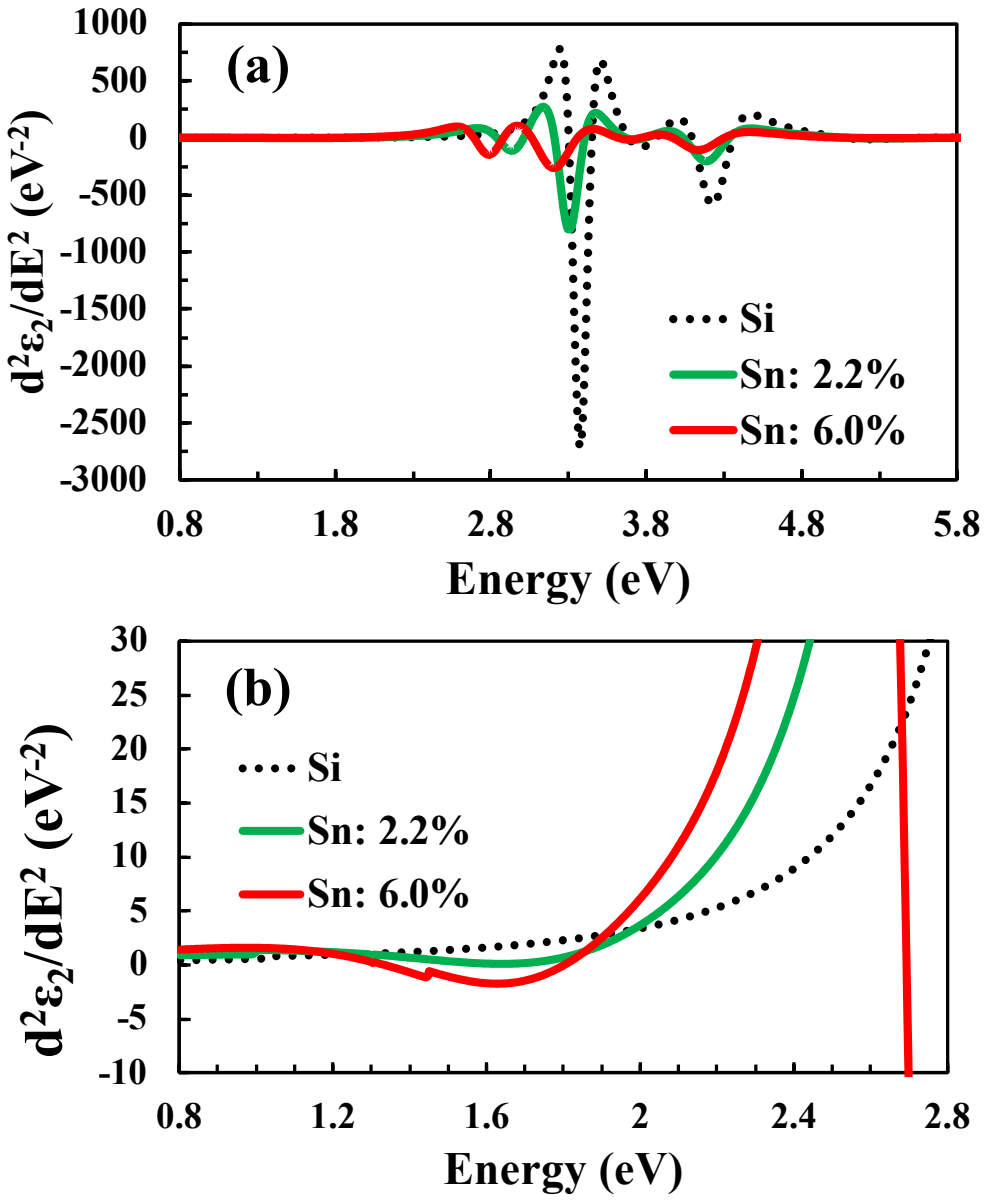

Figure 3. Second derivatives of imaginary part (ε_2) of the complex dielectric function for $Si_{1-x}Sn_x$ (x= 0.022 and 0.06) and pure Si with an energy of (a) 0.8-5.8 eV and (b) 0.8-2.8 eV.

Figure 4 shows Sn fraction dependence of E'_0, E_1, and E_2 in $Si_{1-x}Sn_x$ (x= 0.005 - 0.06) and pure Si obtained from the analysis results. From Fig. 4, it can be confirmed E'_0, E_1, and E_2 peak shifts show the different compositional dependence. Taking into account E'_0, E_1 and E_2 are optical transition around Γ, Λ, and X points, respectively, this result suggests the reduction of band gap with increasing Sn fraction are different at Γ point from the other points. Specifically, coupled with compressive strain and increasing Sn fraction, the band gap at Γ point is reduced more rapidly than those around the Λ and X points, and we consider that compressive strained single crystalline $Si_{1-x}Sn_x$ with high Sn fraction tends to become a direct transition type.

It has been shown in previous reports that split-off of valence band is strongly affected by strain [20]. Therefore, it is expected that the reduction of the band gap is significantly different between unstrained and strained $Si_{1-x}Sn_x$. It is reported that the compressive strain is effective for the reduction of the band gap. In addition, it has also been reported the valence band offset of polycrystalline $Si_{1-x}Sn_x$ is determined by the Sn fraction [21, 22]. We consider those factors led to the Γ point band gap reduction of strained single crystalline $Si_{1-x}Sn_x$. From the above, the band structure of strained single crystal $Si_{1-x}Sn_x$, which had been predicted by theoretical calculations, was experimentally clarified.

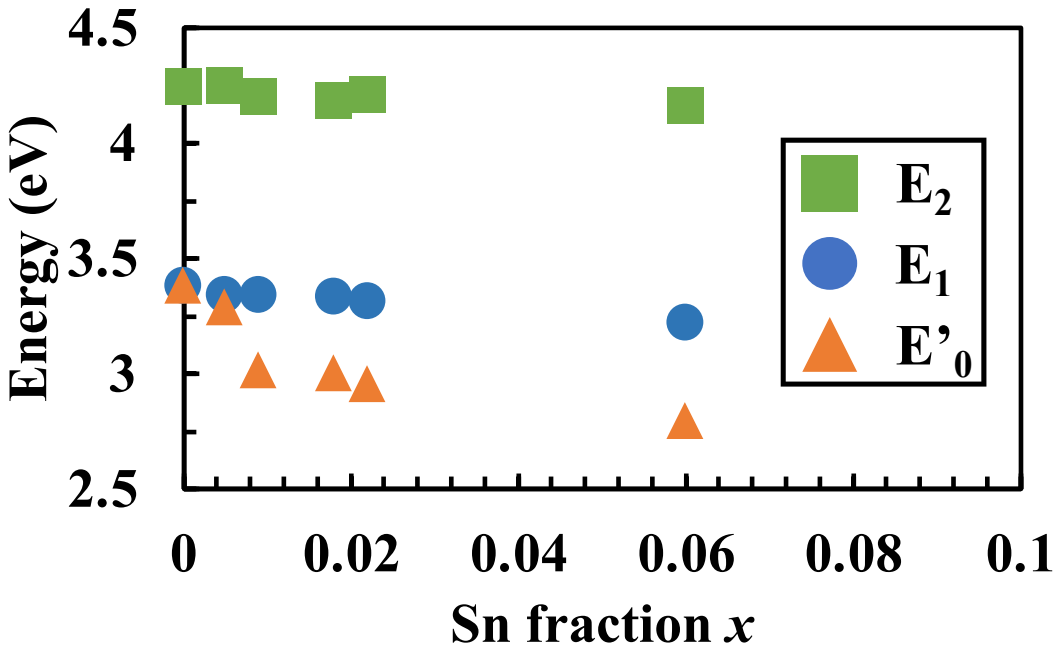

Figure 4. Compositional dependence of (a) E'_0, (b) E_1 and (c) E_2 CP in $Si_{1-x}Sn_x$ (x= 0.005-0.06) and pure Si.

Conclusions

We evaluated the band structure of strained single crystalline $Si_{1-x}Sn_x$ thorough the optical properties using spectroscopic ellipsometry. It was confirmed by the complex dielectric functions for $Si_{1-x}Sn_x$ (x= 0.005 - 0.06) that the two peaks, which are not found in Si, appear for the samples with high Sn composition. We consider a reduction of the band gap at the Γ point and the formation of an optical transition region by Van-Hove singularity due to the Sn addition. Since, as increasing Sn fraction in conjunction with compressive strain, the band gap at the Γ point is reduced more rapidly than those at other points, we predict that the indirect transition type $Si_{1-x}Sn_x$ used in this study may eventually change to the direct transition type. Although higher Sn fraction are required to achieve direct transition type $Si_{1-x}Sn_x$, the band structure of strained single crystal $Si_{1-x}Sn_x$, which had been predicted by theoretical calculations, was experimentally clarified. The results are important findings for the application of SiSn for the near-infrared devices.

Acknowledgment

This work was partly supported by the Japan Society for the Promotion of Science (JSPS) (17J08240, 19K21971, and 21H01366).

References

1. R. A. Soref and C. H. Perry, J. Appl. Phys. **69**, 539 (1991).
2. J. Tolle, A. V. G. Chizmeshya, Y.-Y. Fang, J. Kouvetakis, V. R. D'Costa, C. -W. Hu, J. Menéndez, and I. S. T. Tsong, Appl. Phys. Lett. **89**, 231924 (2006).
3. R. Soref, Opt. Mater. Express **4**, 836 (2014).
4. Y. Nagae, M. Kurosawa, S. Shibayama, M. Araidai, M. Sakashita, O. Nakatsuka, K. Shiraishi, and S. Zaima, Jpn. J. Appl. Phys. **55**, 08PE04 (2016).
5. Y. Nagae, M. Kurosawa, M. Araidai, O. Nakatsuka, K. Shiraishi, and S. Zaima, Jpn. J. Appl. Phys. **56**, 04CR10 (2017).
6. M. Coppinger, J. Hart, and N. Bhargava, Appl. Phys. Lett. **102**, 141101 (2013).
7. P. Moontragoon, Z. Ikonic, and P. Harrison, Semicond. Sci. Technol. **22**, 742 (2007).
8. P. Moontragoon, R. A. Soref, and Z. Ikonic, J. Appl. Phys. **112**, 073106 (2012).
9. D. Girginoudi, N. Georgoulas and A. Thanailakis, J. Appl. Phys. **66**, 354 (1989).
10. T. Nagai, T. Kaneko, Z. Liu, I. Turkevych, and M. Kondo, J. Non-Cryst. Solids. **358**, 2281 (2012).
11. M. Kurosawa, M. Kato, T. Yamaha, N. Taoka, O. Nakatsuka, and S. Zaima, Appl.

Phys. Lett. **106**, 171908 (2015).
12. S. F. Banihashemian, J. M. Grant, A. Sabbar, H. Tran, O. Olorunsola, S. Ojo, S. Amoah, M. Mehboudi, S. Q. Yu, A. Mosleh, and H. A. Naseem, Opt. Mater. Exp. **9**, 2242 (2020).
13. R. Yokogawa, M. Kurosawa, and A. Ogura, ECS Trans. **98**. 291 (2020).
14. C. J. Vineis, Phys. Rev. B. **71**, 245205 (2005).
15. V. R. D'Costa, W. Wang and Y. C. Yeo, J. Appl. Phys. **120**, 063104 (2016).
16. J. Humliček, M. Garriga, M. I. Alonso, and M. Cardona, J. Appl. Phys. **65**, 2827 (1989).
17. D. Imbrenda, R. Hickey, R. A. Carrasco, N. S. Fernando, J. Vanderslice, S. Zollner, and J. Kolodzey, Appl. Phys. Lett. **113**, 122104 (2018).
18. P. Lautenschlager, M. Garriga, L. Vina, and M. Cardona, Phys. Rev. B **36**, 4821 (1987).
19. V. G. Kravets A. N. Grigorenko, R. R. Nair, P. Blake, S. Anissimova, K. S. Novoselov, and A. K. Geim, Phys. Rev. B **81**, 155413 (2010).
20. J. C. Hensel, and G. Feher, Phys. Rev. **129**, 1041 (1963).
21. M. Kurosawa, M. Kato, K. Takahashi, O. Nakatsuka, and S. Zaima, Appl. Phys. Lett. **111**, 192106 (2017).
22. M. Kurosawa, Y. Inaishi, R. Tange, M. Sakashita, O. Nakatsuka, and S. Zaima, Jpn. J. Appl. Phys. **58**, SAAD02 (2019).